Condition Monitoring of High-Sided Tractor-Trailer Units under Gusty Crosswind Conditions

Abubaker Abdulwahab*[1], Rakesh Mishra[2]
[1,2] School of Computing & Engineering, University of Huddersfield, Queensgate, Huddersfield, HD1 3DH, UK

ABSTRACT

It is well established that under gusty crosswind conditions, vehicle aerodynamic forces can lead to sudden changes in vehicle dynamics and stability. Large class vehicles, in particular, are more prone to rollover accidents in strong crosswind situations, especially at cruising speeds. It is therefore essential to conduct detailed investigations on the aerodynamic performance of commercial vehicles under crosswind conditions in order to improve their crosswind stability. This study predicts unsteady aerodynamic forces on a high-sided tractor-trailer unit exposed to gusty crosswind conditions. Although natural wind gusts are highly stochastic phenomena, and have a large variability in types and origins, this investigation suggests using deterministic gust model in combination with Computational Fluid Dynamics (CFD) based approach, using Large Eddy simulation (LES) for modeling air turbulence. Crosswind scenario with gusts of exponential shape, as specified in the Technical Specification for Interoperability (TSI), has been presented in the present study. A series of time-dependent aerodynamic interactions on the tractor-trailer unit have been recorded and investigated through the visualization of instantaneous gust flow structures around the truck-trailer unit. The results show that the TSI gust scenario has significant unsteady effects on the side aerodynamic force and the roll moment of the vehicle. Furthermore, there are significant variations in aerodynamic loads, consistent with the gust's strength.

Key words: Modelling, CFD, Deterministic gust

Corresponding author: Abubaker Abdulwahab (email: Abubaker.Abdulwahab@hud.ac.uk*)*

1. INTRODUCTION

The real atmospheric wind to which a ground vehicle is subjected during on-road driving is fully turbulent and unsteady. Within a turbulent wind field, strong wind pulses can occur and they are known as wind gusts or, more simply, gusts. Under crosswind gust conditions, sudden variations in wind loads have adverse impacts on the dynamic stability of road vehicles[1]. For instance, the aerodynamic roll moment works against vehicle weight loads, thus increasing the risk of rollover or derailment [2]. Therefore, for improving crosswind stability of ground vehicles under gusty wind actions, unsteady vehicle aerodynamic forces are among the essential information needed to carry out the investigation[3].

Modelling wind gust event is a complex task since in the very short-term, the gust speed estimation becomes infeasible. However, for design purposes, gusty wind condition can be evaluated based on the constrained simulation [4]. In this approach, extreme gusts are usually idealized as a deterministic gust, and then the gust is superposed to wind turbulent fluctuations[5]. Also, the deterministic gust model generally describes the stochastic character of the turbulence with the shape of occasional occurring wind peaks[6].

Gust models centered on deterministic approach are applied in various technical and scientific fields. In the rail vehicles area, a large European research projects TRANSAERO[7]and the DEUFRAKO crosswind program[8] contributed to standards in the form of the Technical Specification for Interoperability (TSI) [9,10]. According to these standards, the wind scenario prescribes a deterministic wind gust based on a bi –exponential function, also known as "Chinese hat". A number of studies have utilized the TSI gust scenario to produce the extreme wind loads on rail vehicles (e.g. [5], [11]and [12]).

Once the wind speed time-history is produced as deterministic gust scenario, extreme wind loads on a vehicle are usually expressed through aerodynamic coefficients as [13]:

$$F(t) = \frac{1}{2}\rho_{air} A_r C_i V_{rel}^2(t), i = D,S,L \quad (1)$$

$$M_{x,y,z}(t) = \frac{1}{2}\rho_{air} A_r h C_{mi} V_{rel}^2(t), i = D,S,L \quad (2),$$

where F is a generalized aerodynamic force and M is a generalized aerodynamics moment, ρ_{air} is the air density, A_r is a reference area and h is a reference height. The aerodynamic coefficients are for drag force C_D, lift force C_L, and side force C_S. In Eq. (2) the coefficients are rolling moment coefficient (C_{mD}), pitching coefficient (C_{mS}) and yawing coefficient (C_{ML}). The wind speed relative to the vehicle (Vrel) can be defined directly as a function of the absolute wind speed time-history u(t) seen by the vehicle with velocity of V_{tr}, and it is defined as[3]:

$$V_{rel}^2(t) = (V_{tr} + u(t)\cos\beta)^2 + (u(t)\sin\beta)^2 \quad (3),$$

where β is a wind angle relative to the vehicle moving direction.

Generally, three techniques are conducted for estimating steady and unsteady aerodynamic coefficients of ground vehicles: full-scale measurements, scale model experiments and computational fluid dynamic (CFD) simulations. It is extremely costly and difficult to set up a wind tunnel test that reproduces the ground relative motion [14]. In contrast, CFD computation is well incorporated into the automotive sector and is currently an engineering tool use correspondingly with tests during the aerodynamic design process of ground vehicles [15]. Moreover, the CFD technique can give great quantities of transient data and comprehensive three-dimensional information concerning the wind flow domain [16]. This information can help to elucidate the comprehensive mechanism of the unsteady aerodynamics of road vehicles.

Based on CFD simulation, several techniques were utilized in previous CFD investigations concentrating on turbulent models such as K-ε, K-ω, DES, and LES. However, few examples of using a deterministic gust model in combination with CFD approach can be found in the literature. Favre [15] carried out CFD study to analyses the flow around a simple car geometry under crosswind gust condition. In his investigation, a deterministic wind gust represented by a continuous and smooth step-like function has been used. Vehicle aerodynamic forces were obtained using a commercial software, and the results have been compared against two different types of mesh. His work reveals that deterministic gust models can be applied to simulate crosswind aerodynamic forces on a ground vehicle based on CFD method. However, the study was conducted on a simple small car model, which is less sensitive to the crosswind comparing with trains or high-sided lorries[1]. In addition, the author recommends further investigation based on other types of wind gusts. Similar to [15], a rectangular crosswind profile was considered by Tsubokura et al. [16] . The study carries out a numerical simulation of unsteady aerodynamics of full-scale truck model under wind gust by implementing the LES technique. Numerical values of drag and side coefficients have been validated by wind tunnel tests, and the results show good agreement. However, the maximum gust strength that has been applied was 4.43 m/s, which is relatively small comparing to the strength of the gust in reality.

The TSI wind scenario that has been applied to rail vehicles represents a train traveling on an embankment under constant mean wind load and suddenly being hit by an extreme wind gust[12].This situation applies to road vehicles as well, and from a practical point of view, it is of interest to examine the TSI gust in the road vehicle aerodynamics. Therefore, the present paper is an attempt to use the CFD simulations in combination with the TSI deterministic gust scenarios. The possibility to apply the gust on high-sided trailer is investigated based on the LES turbulent technique. The gust scenario is introduced into the CFD simulation by creating an external velocity data file according to the TSI gust equation and imposing this to the lateral inlet of the computational domain. The

tractor-semitrailer model is fixed on the numerical domain floor, and uniform main flow is imposed at the main inlet, which represents the relative velocity of the surrounding air on the vehicle moving forward in a straight line.

2. METHOD

This section includes a summary of the CFD method that is implemented to analyse the vehicle aerodynamic forces. The CFD simulation was produced using ANSYS-Fluent 17.0 software.

2.1 Vehicle Model and Computational domain

A full-scale model of a tractor semi-trailer based on geometry of real commercial vehicle was developed, and it was adapted by eliminating each small part attached to its surface. As shown in Figure 1, its length, width, and height are 19.03 m, 2.4m, and 4.16m, respectively. The vehicle is anticipated to move directly ahead at a continuous speed of 30 m/s, which is the maximum speed limit for commercial vehicles on highway according to several legislations.

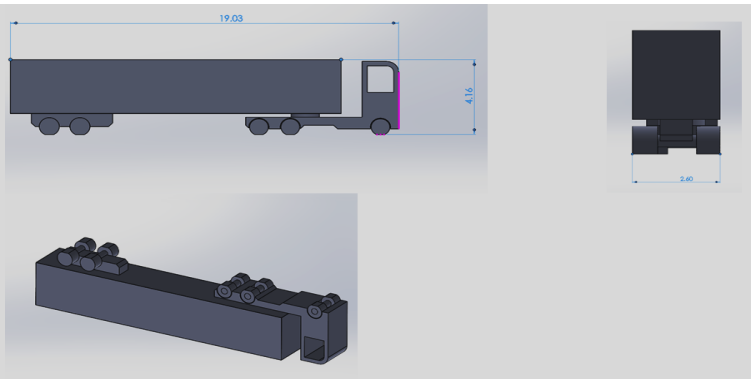

Figure 1: Vehicle 3D CAD model

Further, Figure 2 illustrates a framework of the computational domain used in all CFD analysis presented in this paper. It is expressed as a rectangular duct similar to analysis domain that used in [16], with a 124.5 m length, 126.0 m width, and 32.0 m height. This big domain was implemented to capture the crucial flow features. The domain was split to about 16,250,000 elements with about 2,970,000 vertexes, the number of elements has been chosen after several meshes were tested to check the grid independency. The final mesh was tetrahedral unstructured mesh, this type of mesh has been used in the past for the LES in [16], and the DES in [15], with success. The topology of these control volumes is illustrated in Figure 3. In this figure, two refinement zones are shown, the finest cells zone and the upstream zone. The fine cells are created to capture the small flow structures around the vehicle. Further, a constant time step of $\Delta t = 14 \times 10^{-4}$ s was used to achieve a Courant-Friederich-Lewy (CFL) number beneath 1 so as to acquire a correct and steady solution in this simulation. 20 iterations were performed for each time step to reduce the magnitude of non-linear residuals.

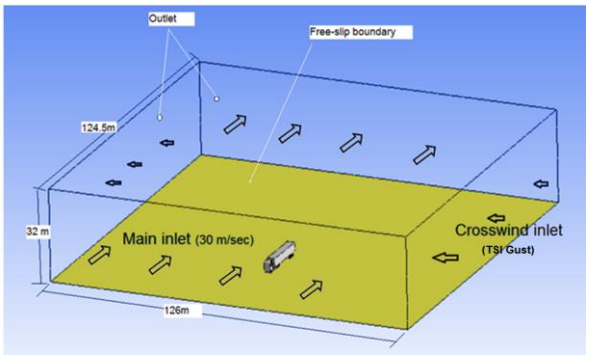

Figure 2: Computational domain and boundary conditions

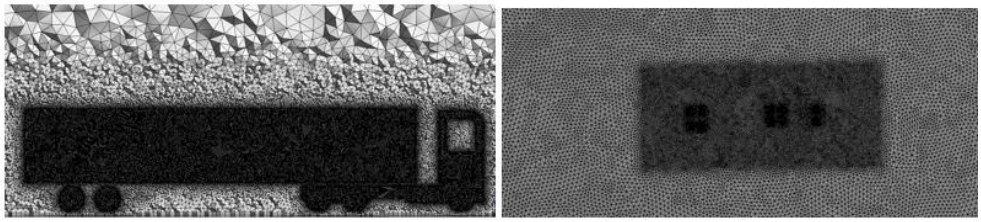

Figure 3: Numerical grids around the truck

2.2 Boundary conditions and boundary data

Figure 2 shows the boundary conditions that used in this investigation. Under these conditions, the truck model is affixed to the floor roughly 40 meters downstream of the domain inlet boundary. The ground is a moving wall with 30 m/s in the streamwise direction, which represents the vehicle speed, and the same speed is applied to the uniform flow at the front inlet. At the outlet faces, zero pressure is arranged, and a symmetry boundary condition is set at the top boundary. As previously mentioned, to reproduce a strong crosswind across the pathway of the truck, the TSI gust profile was imposed on the side boundary of the domain.

2.2.1 TSI Gust-characteristic

The TSI wind gust scenario is developed based on the analysis of real wind data [17]. The full TSI gust scenario (Figure 4) involves a linear rise (from t1 to t2) to the base level of the wind speed ū when the truck semi-trailer is traveling at a consistent state (from t2 to t3). The increase of wind velocity aligns with the exponential gust profile that signifies the wind gust from t3 to t4. Between t4 and t5 the wind velocity reduces to the preceding base level following the gust function. Finally, an additional time stage involving a constant wind speed takes place between t5 and t6.

In a stationary wind speed, the gust is a perturbation velocity, u', added on top of the mean wind speed, $\bar{u}$, depending on the Reynolds decomposition:

$$u(t) = \overline{U} + u'(t) \qquad (4)$$

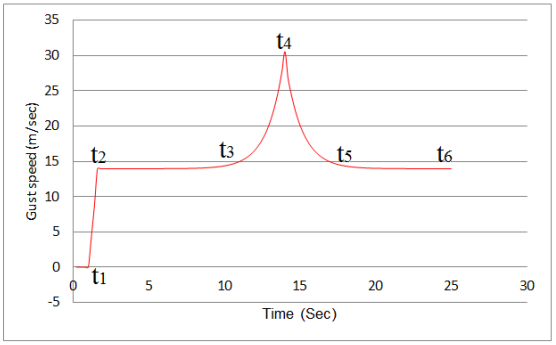

Figure 4: TSI gust scenario

According to the gust modeling methodology in the TSI standard, the perturbation velocity is modeled based on how the mean gust can be described by the autocorrelation function C(t) and amplitude A, i.e u'= A C(t). This leads to a relatively sharp waveform shape; the shape that has been shown to agree with the mean gust obtained from measurements [26]. Thus, wind speed of the bi-exponential profile shown in the Figure (4) is calculated by the following formula [9].

$$u(t) = \bar{u} + \tilde{A}.\sigma_u.C(t) \qquad (5),$$

where the average wind speed and the turbulence intensity determines the standard deviation of longitudinal element (following the average wind speed) of the wind:

$$\sigma_u = I.\bar{u} \qquad (6)$$

The value of normalized gust amplitude ($\tilde{A}$) is fixed by the technique as 2.84. The complex factor in Eq. 5 is the autocorrelation function (C(t)) which represents the correlation between the gust amplitude at the present moment and at the maximum amplitude. This function is formulated by

$$C(t) = \exp\left(-\sqrt{(C_u^x u_x P_u^x)^2 + (C_u^y u_y P_u^y)^2}\right) \qquad (7),$$

where C_u^x and C_u^y are the coherence decay coefficients in the mean wind direction and perpendicular to the mean wind direction respectively; P_u^x and P_u^y are the exponential coefficients in the mean wind direction and perpendicular to the mean wind direction respectively. The values of these coefficients measured experimentally ,and they are given in the TSI standard. After substituting the coefficients values in Eq. 7, the correlation function can be calculated as:

$$C(t) = \exp\left(-\sqrt{(5u_x)^2 + (16u_y)^2}\right) \qquad (8)$$

As the wind gust is fixed in space, the transformation to calculate the temporal distribution is only possible when the vehicle speed is constant [9]. Then , velocity components of the wind along and cross the road are[10]:

$$u_x(\tilde{x}) = \frac{1}{2}\tilde{x}.\cos(\beta).\frac{1}{T.\bar{u}} \qquad (9)$$

$$u_y(\tilde{x}) = \frac{1}{2}\tilde{x}.\sin(\beta).\frac{1}{T.\bar{u}} \qquad (10),$$

where the $\tilde{x}$ term in the equations is a function of the distance along the road towards the position of the maximum amplitude of the gust, and it can be calculated by[9]:

$$\tilde{x} = v_{tr}(t - t_{max}) \qquad (11)$$

Further, by substituting u_x and u_y in Eqs. 8, for β=90 the coherence function is simplified to[10]:

$$C_{(\beta=90)} = e^{16u_x} \qquad (12)$$

2. 3 Governing equations

In principle, the aerodynamic forces are a result of interaction between a vehicle's body and the air surrounding it. To date, LES has been implemented successfully to assess aerodynamics performance of road vehicles , as may be evidenced in the literature (e.g.[3],[16],[14]). In this paper, an incompressible Newtonian fluid was supposed and the equations of continuity and momentum were spatially filtered to acquire the governing equations of LES . For further information on the LES turbulent model see reference[16].

3. SIMULATION RESULTS

For solving the pressure–velocity coupling, the results of the present simulations are obtained with the SIMPLE method. The spatial discretization schemes are a second order for the pressure equation and a bounded central difference for the momentum equation. Also, the bounded second-order implicit scheme is chosen for the transient terms.

3.1 Flow field visualization

In order to discuss trailer crosswind aerodynamic forces and moments, flow field around the trailer predicted in LES analysis is visualized. Figure 5 shows snapshot of gusty wind distribution on a horizontal plane at the mid-height of the trailer, and Figure (6) depicts vortex structures around the truck body. The figures also show values of maximum gust velocity, which corresponding to the maximum gust velocity at 14.6 sec . At the maximum gust speed, the flow accelerates dramatically over the trailer's top and bottom surfaces and through the gap between the tractor and trailer . In addition, the flow separates to form large unsteady structures and fluctuate on both sides of the trailer.

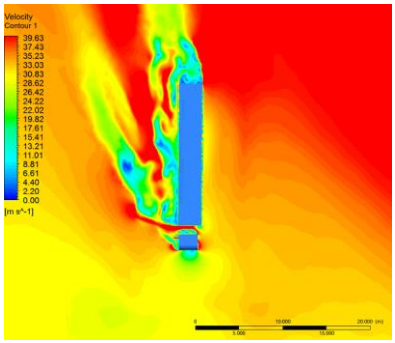

Figure 5: Contour of gust velocity magnitude on a horizontal cut-plane under the TSI gust at t=14.6 sec.

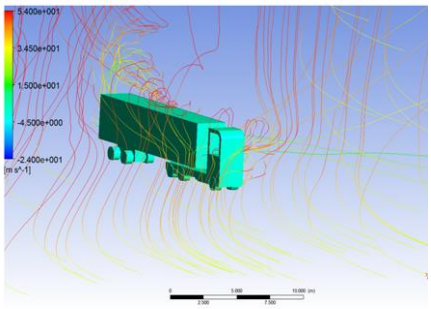

Figure 6: Instantaneous flow structures of the TSI gust around the sides of the trailer at t=14.6 sec.

Contours of the total pressure distributions (Figure 7) have been computed for the leeward and windward sides of the vehicle. Due to the development of flow vortices on the leeward side, a low-pressure region is observed. The existence of the lower pressure region on the leeward side of the train explains the increase in the aerodynamic side force and roll moment. Moreover, high-pressure regions spreads widely on the windward side of the trailer at high speed.

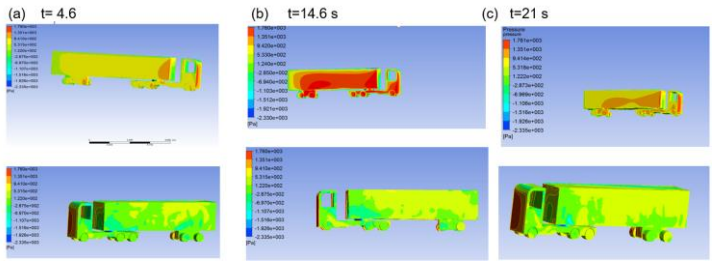

Figure 7: Contours of the total pressure distributions on the truck surfaces under TSI gust scenario (Top windward sides, bottom leeward sides)

3.2 Unsteady aerodynamics loads

Eqs. (1), (2) and (3) were used to calculate the unsteady aerodynamic forces acting on the trailer. Figure 8 illustrates these forces acting on the truck under TSI gust effects. As can be seen from this figure, the aerodynamics force monotonically increase and decrease consistent with the scale of the gust speed. The gust effects observed on the aerodynamic side force is practically about 2.5 times its effects on the drag and lift forces. Also, the vehicle reaches the exponential part of the gust scenario at approximately t=8 seconds, and subsequently, the side aerodynamic force rises from about 11 kN to maximum 33 kN in approximately 6 seconds.

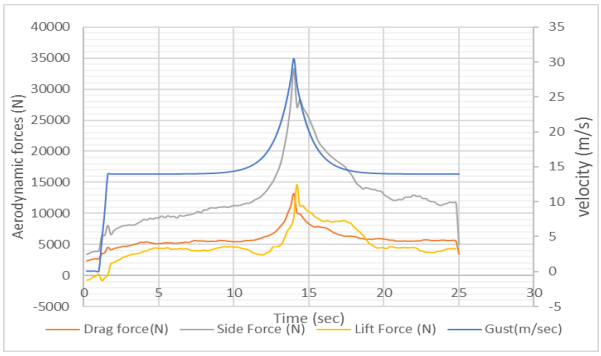

Figure 8: Time history of truck unsteady aerodynamic forces under the effect of the TSI wind scenario.

The gust wind effects can be more visibly perceived in the reaction of aerodynamic moments, Figure (9). Amongst these, the rolling moment displays severe fluctuations, and the yaw moment also displays the penchant of instability. These sudden changes in aerodynamic moments are particularly notable and valuable for the appraisal of vehicular movement stability.

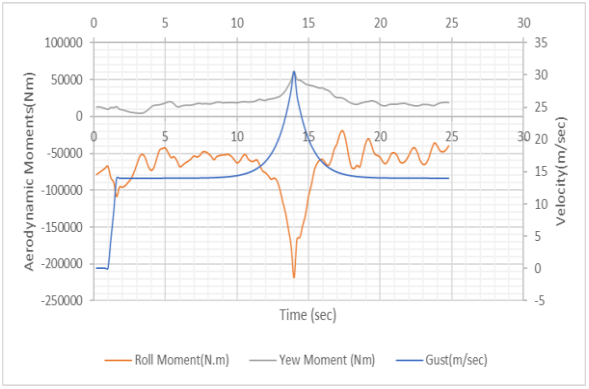

Figure 9: Duration of the unsteady aerodynamic rolling and yawing moments in the TSI wind scenario

4. Conclusion

The TSI gust scenario was applied to the full-scale tractor-semitrailer model in combination with CFD approach. The consequences of unsteady aerodynamics when the vehicle is exposed to this extreme gusty crosswind were predicted. The transient aerodynamic side force and rolling moment were observed to be significantly higher than other aerodynamic forces. Further, throughout the rushing in and out process, variability consistent with the scale of crosswind speed was discovered. These conclusions strongly suggested the significance of considering the unsteady aerodynamic forces in the analysis of heavy vehicle roll dynamics. Moreover, the simulations used in this study were limited to constant gust amplitude. The allowance of varying amplitudes, however, does not result in further problems. Moreover, it appears to be feasible to extend this technique to both bicycles and motorbikes traveling in wind-exposed environments.

REFERENCES

[1] C. Baker, "Ground vehicles in high cross winds part III: The interaction of aerodynamic forces and the vehicle system," Journal of fluids and structures, vol. 5, no. 2, pp. 221-241, 1991.
[2] F. Cheli, F. Ripamonti, D. Rocchi, and G. Tomasini, "Aerodynamic behaviour investigation of the new EMUV250 train to cross wind," Journal of Wind Engineering and Industrial Aerodynamics, vol. 98, no. 4, pp. 189-201, 2010.
[3] C. Baker, F. Cheli, A. Orellano, N. Paradot, C. Proppe, and D. Rocchi, "Cross-wind effects on road and rail vehicles," Vehicle system dynamics, vol. 47, no. 8, pp. 983-1022, 2009.
[4] P. Cheng, and W. Bierbooms, "Extreme gust loading for wind turbines during operation," Journal of Solar Energy Engineering, vol. 123, no. 4, pp. 356-363, 2001.
[5] C. Proppe, and C. Wetzel, "A probabilistic approach for assessing the crosswind stability of ground vehicles," Vehicle System Dynamics, vol. 48, no. S1, pp. 411-428, 2010.
[6] C. Knigge, and S. Raasch, "Improvement and development of one-and two-dimensional discrete gust models using a large-eddy simulation model," Journal of Wind Engineering and Industrial Aerodynamics, vol. 153, pp. 46-59, 2016.
[7] B. Schulte-Werning, A. Deutsche Bahn, F.-u. Technologie-Zentrum, and B. Schulte, "The TRANSAERO Project-Joint European Railway Research on Transient Aerodynamics," TRANSAERO: A European Initiative on Transient Aerodynamics for Railway System Optimisation, vol. 79, pp. 11, 2013.
[8] D. Consortium, "Common DEUFRAKO research on cross wind effects on high speed railway operation 2001–2004," Final Report of DEUFRAKO SIDE WIND project, Draft version, vol. 1, 2004.
[9] O. J. o. t. E. Union, "Technical specification for interoperability," Effects of Crosswinds, 2008.
[10] B. E. 14067-6:2010, "BS EN 14067-6:2010: Railway applications. ," Aerodynamics. Requirements and test procedures for cross wind assessment, Generic, British Standards Institute, 2010.
[11] X. Zhang, Crosswind stability of vehicles under nonstationary wind excitation: KIT Scientific Publishing, 2015.
[12] Wetzel, C., & Proppe, C. (2008, July). Crosswind stability of high-speed trains: a stochastic approach. In *BBAA VI International Colloquium on Bluff Bodies Aerodynamics and Applications, Milano, Italy*.
[13] A. J. Scibor-Rylski, Road vehicle aerodynamics, 1984.
[14] R. McCallen, F. Browand, and J. Ross, The aerodynamics of heavy vehicles: trucks, buses, and trains: Springer Science & Business Media, 2013.
[15] T. Favre, and G. Efraimsson, "An assessment of detached-eddy simulations of unsteady crosswind aerodynamics of road vehicles," Flow, Turbulence and Combustion, vol. 87, no. 1, pp. 133-163, 2011
[16] Tsubokura, K. Takahashi, T. Matsuuki, T. Nakashima, T. Ikenaga, and K. Kitoh, *HPC-LES for Unsteady Aerodynamics of a Heavy Duty Truck in Wind Gust-1st Report: Validation and Unsteady Flow Structures,* 0148-7191, SAE Technical Paper, 2010.
[17] A. Carrarini, "Reliability based analysis of the crosswind stability of railway vehicles," Journal of Wind Engineering and Industrial Aerodynamics, vol. 95, no. 7, pp. 493-509, 2007.